

Bonding in Molecular Clusters and Their Relationship to Bulk Metals*

By D. Michael P. Mingos

INORGANIC CHEMISTRY LABORATORY, UNIVERSITY OF OXFORD, SOUTH PARKS ROAD, OXFORD OX1 3QR

1 Introduction

The remarkable growth in transition metal cluster chemistry which has occurred during the past twenty years represents a major achievement of modern inorganic chemistry.¹ These molecular species have between three and fifty metal atoms bonded together and generally have a protective sheath of ligands bonded to the peripheral metal atoms which makes the clusters inert towards decomposition to the bulk metal.² For the platinum and coinage metals, ligands which are most capable of stabilizing low oxidation states of the metals, *e.g.* carbon monoxide, isocyanides, and phosphines, are particularly effective in blocking such decomposition pathways. For the earlier transition metals, π -donor ligands such as Cl and S stabilize clusters with somewhat higher formal oxidation states. Representative examples of transition metal cluster compounds are summarized in Table 1.³ The characterization of such clusters has also represented a tribute to the power of modern spectroscopic techniques, since even cluster compounds with 44 metal atoms have been structurally defined in the solid state by *X*-ray crystallographic techniques⁴ and, in solution, dynamic aspects of their structural rearrangements have been investigated using Fourier transform n.m.r. and i.r. spectroscopy.⁵ Table 1 also demonstrates that cluster chemistry is not limited to the transition metals, but is also an important feature of main group chemistry. Boron and carbon form an extensive series of polyhedral molecules of the type $B_nH_n^{2-}$, B_nH_{n+4} , B_nH_{n+6} , and C_nH_n .^{6,7} The heavier main group elements, *e.g.* Bi and Sn, form a unique series of 'naked' metal cluster cations and anions.⁸

The characterization of such large molecular cluster compounds with 50 metal atoms or more means that they are approaching the size which one usually associates with crystallites of metals. Such crystallites are formed in finely dispersed

* This review was developed from an Irvine Review Lecture given at St. Andrews University on 9th November 1984.

¹ E. L. Muetterties, *Chem. Eng. News*, 30th August, 1982, 28.

² J. A. Connor in 'Transition Metal Clusters', eds. B. F. G. Johnson, Wiley, New York, 1981, p. 345. Gives an account of the thermodynamic considerations in molecular cluster compounds.

³ E. L. Muetterties, T. N. Rhodin, E. Brand, C. F. Bruker, and W. R. Pretzer, *Chem. Rev.*, 1979, **79**, 91.

⁴ P. R. Raithby in *ref.* 2, p. 5. Gives a summary of *X*-ray crystallographic results on molecular clusters.

⁵ S. Martinengo, B. T. Heaton, R. J. Goodfellow, and P. Chini, *J. Chem. Soc., Chem. Commun.*, 1977, 39.

⁶ 'Boron Hydride Chemistry', ed. E. L. Muetterties, Academic Press, New York, 1975.

⁷ R. J. Ternansky, D. W. Balogh, and L. A. Paquette, *J. Am. Chem. Soc.*, 1982, **104**, 4503 and references therein.

⁸ J. D. Corbett, *Prog. Inorg. Chem.*, 1976, **21**, 129.

Table 1 Some representative examples of molecular cluster compounds

	Type of ligand	Examples	Comments
TRANSITION METAL	Halide and sulphide	$[\text{Mo}_6\text{Cl}_8]^{4+}$ $[\text{Ta}_6\text{Cl}_{12}]^{2+}$	Octahedra of metal atoms d^3, d^4 configurations Rings, deltahedra, and three-connected polyhedra, d^8-d^{10} and $d^{10}s^1$ configurations
	Carbonyl	$[\text{Ir}_4(\text{CO})_{12}]$	
	Phosphine	$[\text{Pt}_3(\text{CO})_3(\text{PR}_3)_3]$ $[\text{Au}_6(\text{PPh}_3)_6]^{2+}$	
MAIN GROUP	Hydride and alkyl	$[\text{B}_6\text{H}_6]^{2-}$, C_8H_8	Deltahedra and three-connected polyhedra, s^2p^1 and s^2p^2 configurations
	'Naked metal clusters'	$[\text{Sn}_9]^{2-}$	

metal catalysts and *via* the aggregation of metal atoms in low temperature matrices.⁹ The study of such crystallites which have diameters less than 100 Å poses great experimental difficulties because of unavoidable particle size distributions within a particular sample and the necessity for high vacuum techniques to ensure that contamination of the surfaces of the particles does not occur.¹⁰ Since these problems do not arise for molecular cluster species they provide a way of studying some fundamental questions concerning the evolution of properties from the molecular to the bulk states.

The valency problems raised by the occurrence of such an extensive and complex range of chemical compounds are considerable and the large number of metal atoms puts this class of compound beyond the range of *ab initio* calculations. Nevertheless, the combination of semi-empirical molecular orbital calculations and symmetry arguments has led to some important generalizations which relate the observed structures of simple clusters to their polyhedral skeletal geometries.¹¹⁻¹⁵ In addition they have demonstrated how the bonding requirements of these clusters change as they are condensed into larger aggregates by means of vertex, edge, and face sharing processes.¹⁶ For high nuclearity clusters the bonding must begin to approach that observed for the bulk metal and therefore clusters provide an opportunity for studying the development metallic properties.¹⁷

To emphasize the relationship between clusters and the bulk metals the bonding

⁹ J. P. Borel and J. Buttet, *Surf. Sci.*, 1981, **106**, 1.

¹⁰ S. C. Davis and K. J. Klabunde, *Chem. Rev.*, 1982, **82**, 153 and G. A. Ozin, *Faraday Symp. Chem. Soc.*, 1980, **14**, 7.

¹¹ R. E. Williams, *Inorg. Chem.*, 1971, **10**, 210.

¹² K. Wade, *J. Chem. Soc., Chem. Commun.*, 1971, 792.

¹³ K. Wade, *Adv. Inorg. Chem. Radiochem.*, 1976, **18**, 1.

¹⁴ D. M. P. Mingos, *Nature (London), Phys. Sci.*, 1972, **236**, 99.

¹⁵ D. M. P. Mingos, *Acc. Chem. Res.*, 1984, **17**, 311.

¹⁶ D. M. P. Mingos, *J. Chem. Soc., Chem. Commun.*, 1983, 706.

¹⁷ R. E. Benfield, P. P. Edwards, W. J. H. Nelson, M. D. Vargas, D. C. Johnson, and M. J. Sienko, *Nature (London)*, 1985, **314**, 231.

characteristics of the metal d , s , and p orbitals in the former will be described using the band type of nomenclature used for infinite solids.¹⁸ The bonding description also relies heavily on the ideas and notation developed by Stone in his Tensor Surface Harmonic Theory.^{19,20} Such a description is applicable to all classes of cluster given in Table 1 and serves to emphasize their similarities and differences.

2 'Band' Description of the Bonding in Clusters

High nuclearity molecular clusters have a large number of molecular orbitals whose energies are closely spaced and therefore it becomes cumbersome to specify the degeneracies, symmetries, and energies of all the levels. It is more economical to envisage the cluster molecular orbitals generated from the nd , $(n + 1)s$, and $(n + 1)p$ valence orbitals as related to the type of band of molecular orbitals used to describe the bonding in infinite arrays of metal atoms. In this way it is not necessary to identify all the components of the band, but merely the predominant bonding characteristics and the band widths. These depend on the nodal characteristics of the atomic orbitals contributing to the band and their mutual overlaps.

A. d -Band.—The $5m$ d valence orbitals of a naked transition metal cluster, M_m , generate a closely spaced set of molecular orbitals with an overall band width of *ca.* 1.5—4.0 eV.²¹ The band width narrows across the transition series as the effective nuclear charge of the metal increases. For the post transition metals these orbitals effectively enter into the core and make little contribution to metal–metal bonding. For a particular cluster the molecular orbitals become progressively more antibonding as the band is ascended and therefore maximum metal–metal bonding is achieved for a half filled band and the interactions are overall repulsive for a filled band, *i.e.* for a d^{10} cluster.

If local co-ordinate systems with the z axes pointing towards the centre of the cluster are chosen the d_z^2 orbitals are cylindrically symmetric and are described as d^{σ} orbitals. The d_{xz} and d_{yz} orbitals have a single nodal plane containing the radius vector and are described as d^{π} , and d_{xy} and $d_{x^2-y^2}$ have two nodal planes and are described as d^{δ} (see Figure 1).¹⁹ The d^{σ} orbitals generate a set of molecular orbitals S_d^{σ} , P_d^{σ} , $D_d^{\sigma} \dots L_d^{\sigma}$, whose energies increase with the number of nodes, *i.e.* S_d^{σ} is the most stable and represents an in-phase combination of all d^{σ} orbitals, P_d^{σ} has a maximum degeneracy of three with each component having a single node, *etc.*¹⁹ In M_m there are a total of m L_d^{σ} molecular orbitals, and their relative energies are represented schematically in Figure 1. In a spherical cluster the d^{π} and d^{δ} orbitals generate pairs of m bonding and m antibonding molecular orbitals, L^{π} , $L^{\bar{\pi}}$, L^{δ} , $L^{\bar{\delta}}$, which are related by a parity transformation operation.¹⁹ This operation, which is illustrated in Figure 2, rotates each of the local d^{π} or d^{δ} orbitals by 90° in a clockwise fashion. This rotation has the effect of transforming a bonding molecular orbital into a molecular orbital which is equally antibonding. There are a total of

¹⁸ 'Chemical Structure and Bonding', R. L. DeKock and H. B. Gray, Benjamin/Cummings, Menlo Park, California, 1980, p. 419.

¹⁹ A. J. Stone, *Mol. Phys.*, 1980, **41**, 1339; *Inorg. Chem.*, 1981, **20**, 563.

²⁰ A. J. Stone and M. J. Alderton, *Inorg. Chem.*, 1982, **21**, 2297.

²¹ R. G. Wooley in 'Transition Metal Clusters', ed. B. F. G. Johnson, Wiley, New York, 1980, 607.

$4m$ d^n and d^{δ} functions, $2m$ of which form a bonding band and $2m$ an antibonding band (see Figure 1).

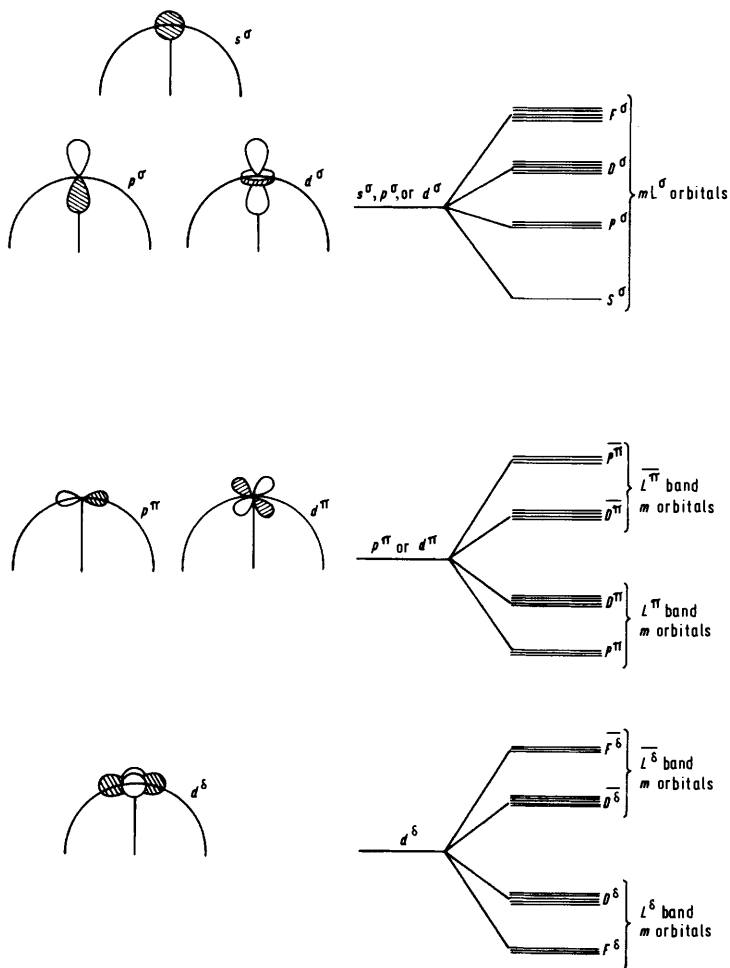


Figure 1 Designation of nodal characteristics of l^{σ} ($l = s, p,$ and d), l^{π} ($l = p$ or d), and d^{δ} atomic orbitals on the surface of a spherical cluster. The nodal planes are referenced to the radius vector of the cluster

For metal halide and sulphide clusters of the earlier transition metals with d^3 — d^5 electronic configurations the d band is partially filled and the occurrence of strong metal–metal bonding in clusters such as $[\text{Ta}_6\text{Cl}_{12}]^{2+}$ and $[\text{Mo}_6\text{Cl}_8]^{4+}$ is consistent with a partial filling of the d band. In metal carbonyl clusters where the metals generally have d^8 — d^{10} configurations the occurrence of strong metal–metal

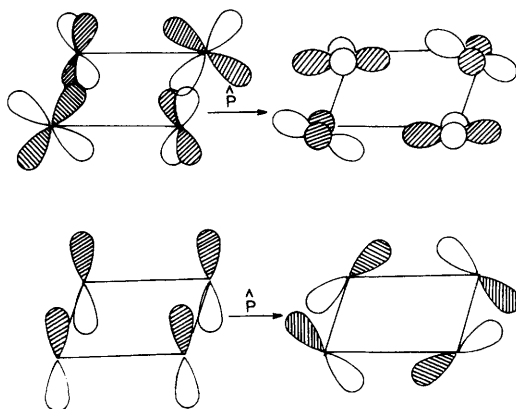


Figure 2 The parity transformation operation \hat{P} has the effect of changing a bonding molecular orbital into an equally antibonding molecular orbital

bonding cannot be attributed to bonding effects within the d band. Two factors serve to reduce the extent of antibonding character of the filled d band. First, mixing in of s character from the higher lying s band reduces the antibonding character of the L_d^σ orbitals at the top of the band; second, the ligands co-ordinated to the cluster cause a redistribution of electron density. For the later transition metals, carbonyl and related π -acceptor ligands stabilize the clusters by transferring electron density preferentially from the filled antibonding components of the d band to empty π -acceptor levels of the ligand. This preferential effect arises because the acceptor levels are higher lying than the d band and interact more strongly with the more antibonding components where the energy match is better.²²

B. s -Band.—For the earlier transition metals the $(n + 1)s$ valence orbitals are rather diffuse and give rise to bands which in the bulk metal would approximate to a free electron distribution. Although the band width is much wider than that for the d orbitals, the overall contribution to bonding is diminished because the orbitals have significant probabilities in core regions of adjacent metal atoms.²¹ Across the transition series the increase in nuclear charge contracts the s orbitals and for the later transition metals, platinum and gold for example, and for the post transition metals, the $(n + 1)s$ orbitals make a significant contribution to metal–metal bonding. Contraction of the s orbitals resulting from relativistic effects is particularly important for the heavier transition metals and leads to a strengthening of metal–metal bonding.^{23,24} In metal clusters where the metal atoms are distributed in an approximately spherical fashion the s orbitals generate the $S_s^\sigma, P_s^\sigma, D_s^\sigma \cdots L_s^\sigma$ cluster molecular orbitals shown in Figure 1 in much the

²² R. L. Johnston and D. M. P. Mingos, *Inorg. Chem.*, in press.

²³ K. S. Pitzer, *Acc. Chem. Res.*, 1979, **12**, 271.

²⁴ P. Pykkö and J. P. Desclaux, *Acc. Chem. Res.*, 1979, **12**, 276.

same way as described above for the d^σ orbitals. When the number of metal atoms exceeds six then the S_s^σ and P_s^σ molecular orbitals are bonding and the remaining functions are antibonding.¹⁹

C. p -Band.—The $(n + 1)p$ valence orbitals are also very diffuse and lead to broad bands particularly for the earlier transition metals. These molecular orbitals contribute even less to bonding in transition metal clusters because the s — p promotion energies are substantial and only make a significant contribution to metal—metal bonding for the post transition metals. However, even for the earlier transition metals, they play an important role in influencing the stoichiometries and structures of metal clusters by acting as acceptors to the bridging and terminal ligands.

Using the local co-ordinate system defined previously, the p_z orbitals (described as p^σ) give rise to a set of $m S_p^\sigma, P_p^\sigma, D_p^\sigma \dots L_p^\sigma$ molecular orbitals, which when hybridized with the lower lying L_s^σ functions act effectively as acceptor functions for ligands which are bonded to the cluster in a radial fashion. The $p_x, p_y, (p^\pi)$ orbitals generate pairs of L_p^π and \bar{L}_p^π molecular orbitals related by the parity transformation.¹⁹ The relative bonding character of these molecular orbitals are illustrated schematically in Figure 1.

In a molecular cluster the metal contributes $nd, (n + 1)s$, and $(n + 1)p$ valence

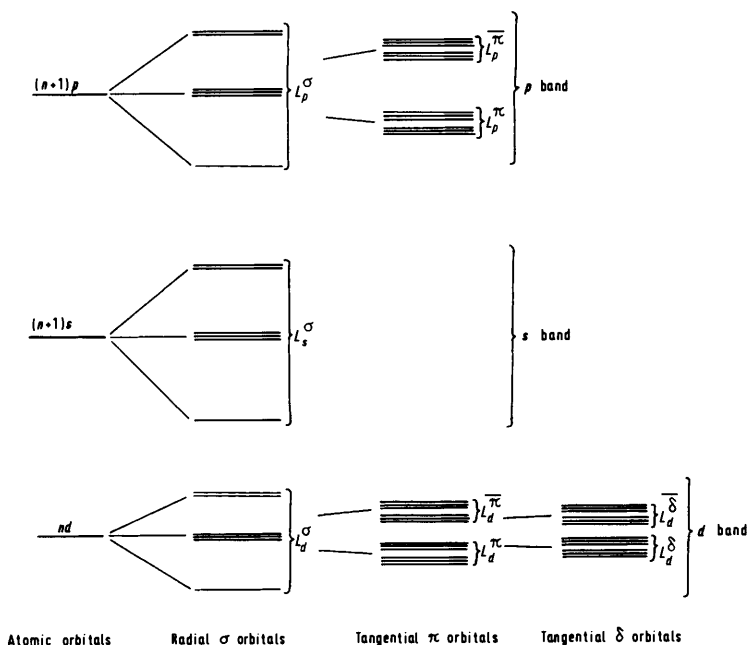


Figure 3 Schematic representation of the $d, (n + 1)s$, and $(n + 1)p$ bands for a spherical molecular cluster

orbitals and the relative energies of these orbitals are represented schematically in Figure 3. Some mixing must occur between orbitals of the same symmetry, but derived from different atomic orbitals. Stone's Surface Harmonic Theory allows one to classify the orbitals according to the approximate spherical symmetry and thereby to reduce greatly the number of orbitals which need to be considered. The extent of mixing also depends critically on the relative energies of the nd , $(n + 1)s$, and $(n + 1)p$ valence orbitals. The supplementary mixings which occur between the various components of the bands are discussed below with reference to specific classes of cluster molecules.

3 Specific Classes of Cluster Compounds

A. 'Naked' Clusters of the Post Transition Metals.—For the post transition metals the d band is effectively part of the core and the s orbitals in clusters of tin and bismuth, for example, give rise to a relatively narrow band of $m L_s^\sigma$ levels, which in a localized bonding picture would correspond to lone pairs on each of the metal atoms. The metal-metal bonding occurs primarily through the p valence orbitals, simplifying the bonding situation considerably. The geometry of the cluster determines the spectrum of levels which constitute the bands derived from p^σ and p^π . For deltahedral clusters the number of nearest neighbour interactions are maximized leading to a very stable S_p^σ molecular orbital and $m L_p^\pi$ tangential bonding molecular orbitals (see Figure 4). The remaining $(m - 1)L_p^\sigma$ radial and $m L_p^\pi$ molecular orbitals are generally unavailable for bonding because of their antibonding character. The unequal distribution of bonding and antibonding molecular orbitals, *i.e.* $m + 1$ bonding and $2m - 1$ antibonding arises because of the multicentred nature of the bonding in these deltahedra. If the filled d and s bands are included in the valence electron count for these deltahedral clusters they are characterized by a total of $7m + 1$ electron pairs ($2m + 1$ if the d band is excluded).

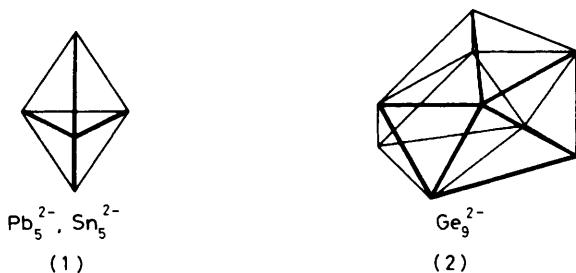
Examples of such clusters include:²⁵ Pb_5^{2-} and Sn_5^{2-} , trigonal bipyramid (1), and Ge_9^{2-} , tricapped trigonal prism (2). In (2) detailed molecular orbital calculations have shown that the picture described above represents a slight oversimplification because the more antibonding components of the L_p^π band and the more bonding components of the $\overline{L_p^\pi}$ band merge.²⁶ In particular, the $\overline{F_0^\pi}(a_2')$ component lies at slightly lower energies than $F_0^\pi(a_2'')$. Occupation of the former leads to an electron count of 128 ($7m + 1$ orbitals), *e.g.* Ge_9^{2-} , and the latter 130, *e.g.* Sn_9^{4-} and Bi_9^{5+} .²⁷ Interestingly, the latter show structural distortions consistent with the occupation of an orbital of a_2'' symmetry which is antibonding between the triangular faces of the central trigonal prism.

The adoption of three-connected polyhedra, which minimize the number of next neighbour interactions, leads to a different spectrum of molecular orbitals for the

²⁵ P. E. Edwards and J. D. Corbett, *Inorg. Chem.*, 1977, **16**, 903; C. H. E. Belin, J. D. Corbett, and A. Cisar, *J. Am. Chem. Soc.*, 1977, **99**, 7163; S. C. Critchlow and J. D. Corbett, *Inorg. Chem.*, 1982, **21**, 3286.

²⁶ K. Wade and M. E. O'Neill, *Polyhedron*, 1983, **2**, 5715; S. J. Critchlow and J. D. Corbett, *J. Am. Chem. Soc.*, 1983, **105**, 5115.

²⁷ R. L. Johnston and D. M. P. Mingos, *J. Organomet. Chem.*, 1985, **280**, 407.



band derived from the p^π orbitals in these naked clusters. In particular, these polyhedra are characterized by a strongly bonding set of $[(m/2) + 1]$ molecular orbitals derived from the L_p^π band, and $(m - 2)$ approximately non-bonding molecular orbitals derived equally from L_p^π and L_p^π which are matched by the parity

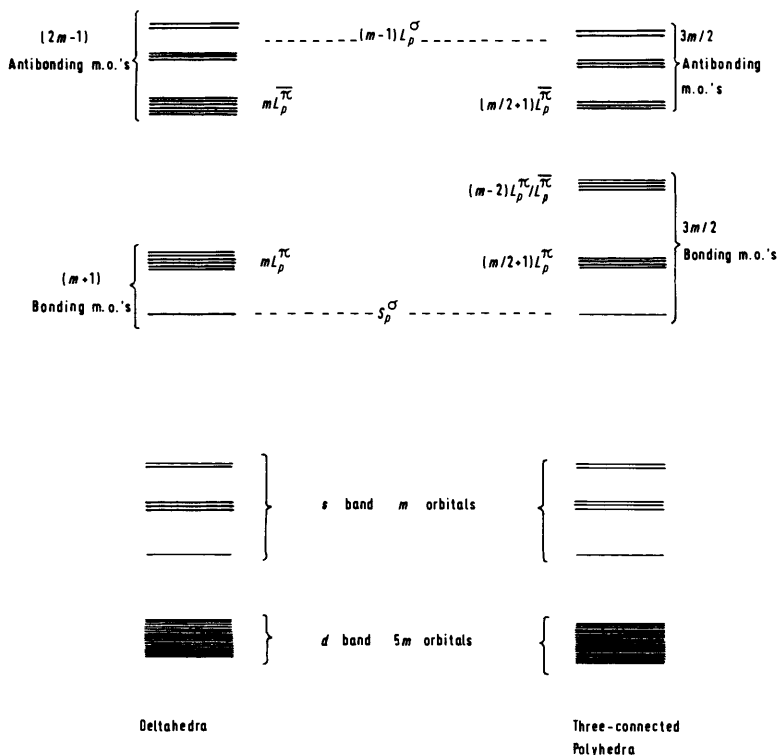


Figure 4 A general representation of the molecular orbitals in 'naked' metal clusters of the post transition metals. The diagram excludes P_p^σ and P_d^π mixings which m.o. calculations have shown to be important

transformation operation. $[(m/2) + 1]$ strongly antibonding molecular orbitals derived from L_p^π and $(m - 1)L_p^\sigma$ antibonding radial molecular orbitals complete the spectrum of molecular orbitals shown in Figure 4. The symmetric distribution of molecular orbitals in such clusters means that the $3m/2$ bonding skeletal molecular orbitals can be described also in terms of localized bonding schemes.²⁷ Occupation of the d and s bands and the bonding molecular orbitals described above leads to a total of $15m/2$ accessible molecular orbitals. Examples of such bare metal clusters include $\text{Sn}_2\text{Bi}_2^{2-}$ and Sb_4 , both of which have tetrahedral geometries and a total of 60 valence electrons if the d band is included.²⁵ Higher nuclearity three-connected naked metal clusters with $15m$ valence electrons represent an interesting synthetic goal.

B. Borane and Hydrocarbon Polyhedral Molecules.—For the lighter main group elements the s — p promotion energies are smaller and considerable mixing between the L_s^σ and L_p^σ bands occurs leading to sets of radial molecular orbitals which are either hybridized in towards or away from the centre of the cluster. Consequently

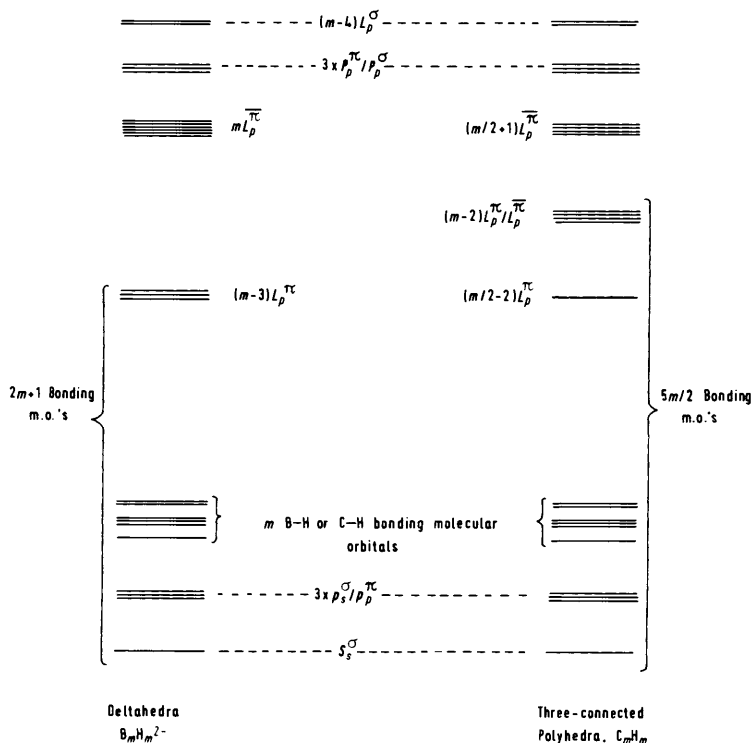


Figure 5 Schematic representations of the molecular orbitals in deltahedral and three-connected molecular clusters $E_m H_m$ ($E = B$ or C)

bare metal clusters are not observed for these elements and clusters of boron and carbon, for example, are observed only when there are groups attached to them in a terminal fashion. The terminal ligands (usually H or an organic radical R) donate electrons into the outpointing components of the L_s^σ/L_p^σ band and generate the set of m bonding B–H molecular orbitals shown in Figure 5. Therefore, the bonding situation is closely related to that described above for bare metal clusters. However, in these clusters the degree of mixing between radial and tangential bonding components is more obvious. In particular, the most stable component of the L_p^π band, P_p^π , mixes extensively with P_s^σ from the L_s^σ band and generates a strongly bonding component P_s^σ/P_p^π . The total number of bonding skeletal molecular orbitals remains the same, $(m + 1)$ in a deltahedron and $3m/2$ in a three-connected polyhedron.²⁸

There exists an extensive series of borane anions, $B_mH_m^{2-}$, with deltahedral geometries with $4m + 2$ valence electrons and three-connected hydrocarbon polyhedra with $5m$ valence electrons. Examples of such molecules are summarized in Table 2^{6,7} and Figures 6 and 7.

The borane polyhedral molecules also have important sub-groups of polyhedra

Deltahedral boranes with $4m + 2$ valence electrons

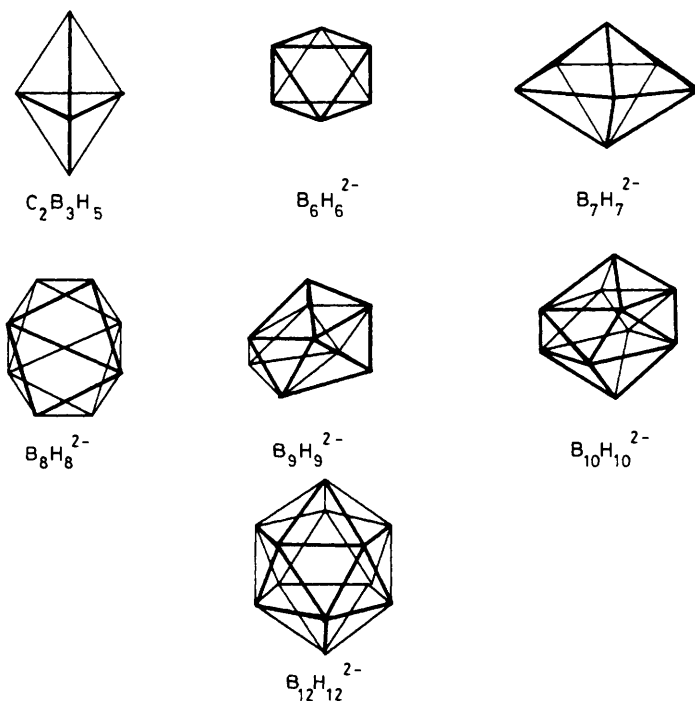


Figure 6 Some examples of deltahedral boranes and carboranes

Three-connected hydrocarbon polyhedra with $5m$ valence electrons

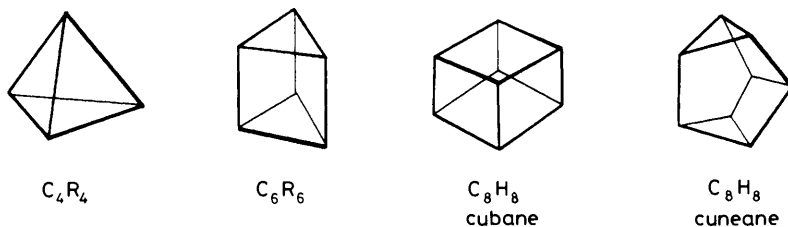


Figure 7 Some examples of three-connected hydrocarbon polyhedral molecules

Table 2 Summary of polyhedral electron counts for main group polyhedral molecules

	Main Group Hydrides	Examples	Naked Metal Clusters (With filled d shell)	Examples
<i>closo</i> -Deltahedra	$4m + 2$ ($m \geq 5$)	$B_mH_m^{2-}$	$14m + 2$	Ge_9^{2-}
<i>nido</i> -Deltahedra	$4m + 4$ ($m \geq 4$)	B_mH_{m+4}	$14m + 4$	
<i>arachno</i> -Deltahedra	$4m + 6$ ($m \geq 4$)	B_mH_{m+6}	$14m + 6$	Bi_8^{2+} (square antiprism)
Three-connected polyhedra	$5m$ (m even ≥ 4)	C_mH_m	$15m$	Sb_4 (tetrahedron)
Ring compounds	$6m$ ($m \geq 3$)	C_mH_{2m}	$16m$	Sn_4R_8

The number of skeletal electron pairs (M) in a polyhedral molecule is related to the polyhedral electron count (p.e.c.) by $M = [\text{p.e.c.} - 2m]/2$ for main group non-metals and $[\text{p.e.c.} - 12m]/2$ for main group metals

which are derived from the deltahedra by the loss of vertices. The polyhedral cages in these compounds are described as *nido*- if they are related to the parent *closo*-deltahedron by the loss of a single vertex, and *arachno*- if they are related by the loss of two vertices. Some examples of these *closo*-, *nido*- and *arachno*-polyhedral boranes are illustrated in Figure 8. The *nido*-clusters are characterized by $4m + 4$ valence electrons and the *arachno*- by $4m + 6$ valence electrons. These polyhedral molecules frequently have bridging hydrogens around the open faces which topologically compensate for the s and p valence orbitals of the missing vertices.^{11,14}

C. Transition Metal Carbonyl and Related Clusters.—*Clusters with Bonding Components of L_p^*/\bar{L}_p^* Band Filled.* Figure 9 illustrates schematically the bands of molecular orbitals for a transition metal cluster M_mL_m . They bear a remarkable similarity to those described above for main group clusters, but the following important differences need to be emphasized. The d band width is somewhat larger for transition metal clusters because the d orbitals are less core-like. It follows that the d orbitals make a larger contribution to metal-metal bonding as long as the d shell is not completely filled. This is achieved for d^{10} metals by back donation of

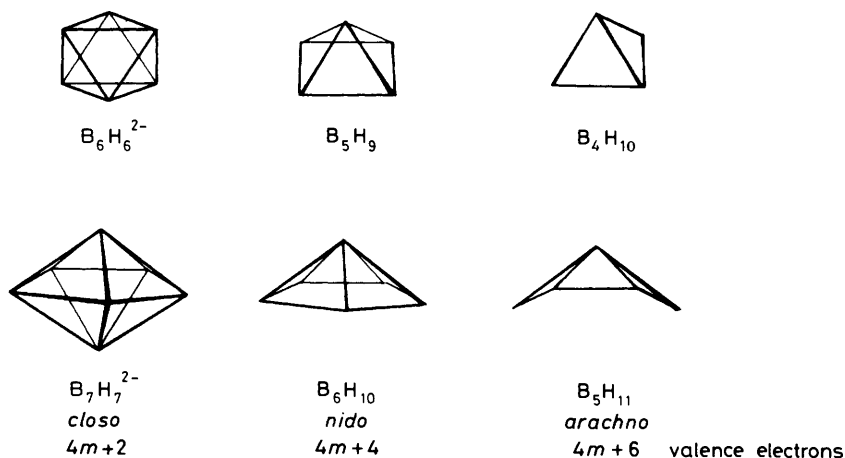


Figure 8 Some simple examples of closo-, nido-, and arachno-polyhedral boranes. For reasons of clarity the hydrogen atoms have been excluded

electron density from the d band into the π^* orbitals of the ligands. For a deltahedral cluster the S_s^σ , P_s^σ/P_p^π , and $(m-3)L_p^\pi$ radial and tangential molecular orbitals resemble those of $B_mH_m^{2-}$, but the L_p^π orbitals cannot contribute directly to bonding because of the large $d-p$ promotion energies. These orbitals can, however, act effectively as acceptor orbitals for those additional ligands which are bonded to the metal either in a terminal or bridging fashion. Complete utilization of these acceptor orbitals will only occur for clusters where the number of additional ligands exceeds the number of acceptor orbitals and the metal $d-p$ promotion energy is not excessively large.²⁸

Under these conditions the main group and transition metal clusters have in common a set of inaccessible orbitals which have a high proportion of p orbital character and which are characteristic of the metal polyhedral geometry.^{19,29} In a transition metal cluster these orbitals are not suitable for accepting electron pairs from the σ orbitals of ligands because they are metal-metal antibonding and have nodes across the edges of the polyhedron. The parity transformation operation illustrated in Figure 2 ensures this nodal characteristic for the \overline{L}_p^π orbitals in a deltahedron. The $(m-4)L_p^\sigma$ orbitals illustrated in Figure 9 are also unsuitable for accepting electron pairs because they are antibonding radial molecular orbitals. A deltahedral metal cluster has mL_p^π , $3P_p^\pi/P_s^\sigma$, and $(m-4)L_p^\sigma$ inaccessible orbitals and is therefore characterized by a total of $7m+1$ orbitals which are involved either in metal-metal bonding or metal-ligand bonding. A three-connected polyhedron has $[(m/2)+1]\overline{L}_p^\pi$, $3P_p^\pi/P_s^\sigma$, and $(m-4)L_p^\sigma$ inaccessible orbitals and consequently is associated with $15m/2$ electron pairs. Some specific examples of deltahedral and three-connected cluster compounds of the transition metals are

²⁸ P. L. Brint, J. P. Cronin, and E. Seward, *J. Chem. Soc., Dalton Trans.*, 1983, 975.

²⁹ D. M. P. Mingos, *J. Chem. Soc., Dalton Trans.*, 1974, 133.

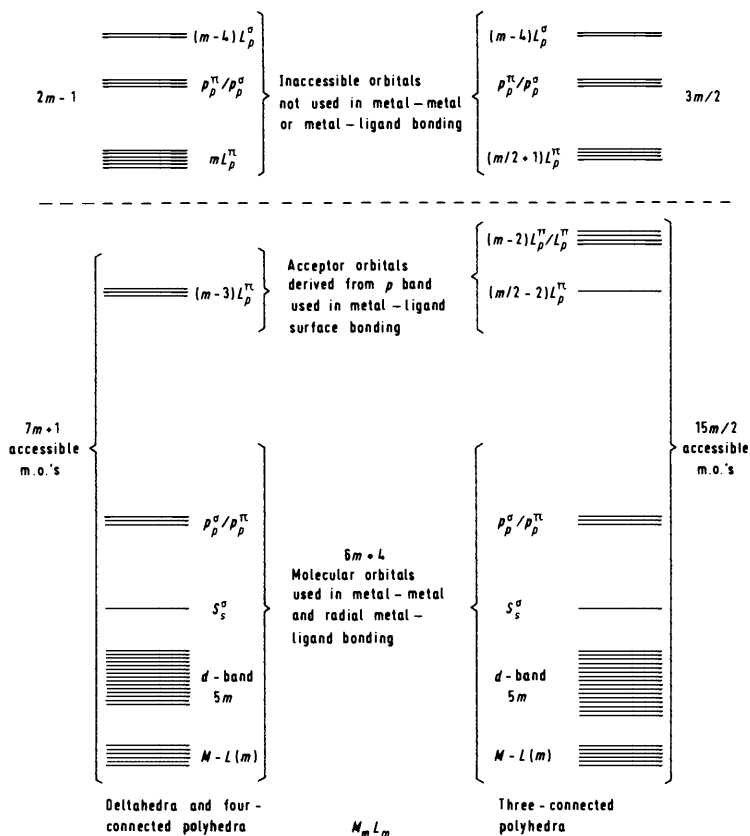


Figure 9 A general representation of the molecular orbitals for deltahedral, four-connected, and three-connected polyhedral molecules of the transition metals. The molecular orbitals are generally occupied up to the dotted line shown in the Figure

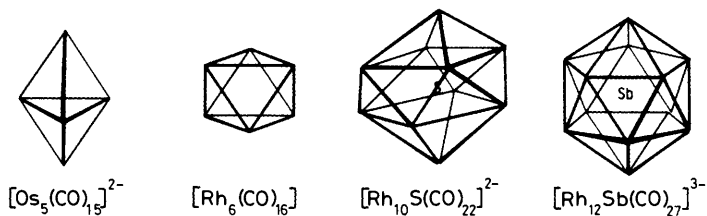
illustrated in Figures 10 and 11 and their general electronic characteristics are summarized in Table 3.¹⁵

Planar cluster compounds based on rings are also known for metal carbonyl clusters. They are characterized by $16m$ valence electrons and some examples are illustrated in Figure 11. The bonding in these ring compounds and the three-connected polyhedral clusters can both be described in terms of localized bonding schemes, with each metal atom achieving an eighteen electron configuration.

The deltahedral and four-connected polyhedral molecules illustrated in Figure 10 are both characterized by $14m + 2$ valence electrons. They cannot be described by localized bonding schemes because of a lack of correspondence between the number of inaccessible orbitals and the number of edges of the polyhedron.³⁰ The

³⁰ R. L. Johnston and D. M. P. Mingos, *J. Organomet. Chem.*, 1985, **280**, 419.

Deltahedral metal carbonyl clusters with $14m+2$ valence electrons



Four-connected metal carbonyl clusters with $14m+2$ valence electrons

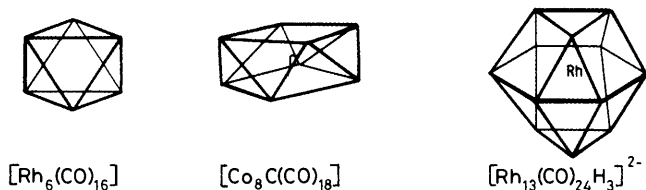
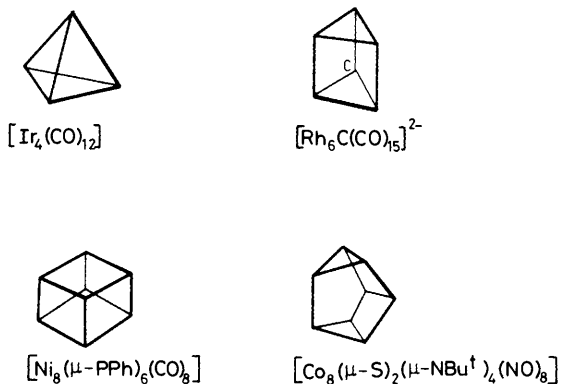


Figure 10 Some examples of deltahedral and four-connected transition metal carbonyl cluster compounds

Three-connected metal clusters with $15m$ valence electrons



Ring cluster compounds with $16m$ valence electrons

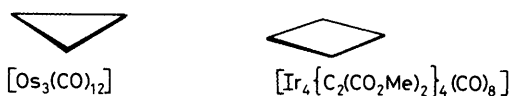


Figure 11 Some example of three-connected and ring compounds of transition metal carbonyls

Table 3 Summary of electronic characteristics of transition metal clusters where radial and tangential bonding effects are structurally important

Polyhedral Description	Characteristic Electron Count	Example
closo-Deltahedron	$14m + 2$	$\text{Os}_5(\text{CO})_{15}^{2-}$ (trigonal bipyramid), $\text{Rh}_6(\text{CO})_{16}$ (octahedron), $[\text{Rh}_{12}\text{Sb}(\text{CO})_{27}]^{3-}$ (icosahedron)
nido-Deltahedron	$14m + 4$	$\text{Ru}_5\text{C}(\text{CO})_{15}$ (square pyramid)
arachno-Deltahedron	$14m + 6$	$\text{Fe}_4\text{H}(\text{CO})_{13}^-$ (butterfly)
Four-connected polyhedron	$14m + 2$	$[\text{Co}_8\text{C}(\text{CO})_{18}]^{2-}$ (square antiprism)
Three-connected polyhedron	$15m$	$[\text{Rh}_6\text{C}(\text{CO})_{15}]^{2-}$ (trigonal prism)
Ring compounds	$16m$	$\text{Os}_3(\text{CO})_{12}$ (triangle)

range of deltahedral metal clusters is much more limited than that observed for borane anions, and currently only trigonal bipyramidal, octahedral, bicapped square-antiprismatic, and icosahedral examples have been characterized. Examples of four-connected transition metal carbonyl cluster compounds include the octahedron, the square-antiprism, and the twinned anti-cuboctahedron.

A notable feature of many of the cluster compounds illustrated in Figures 10 and 11 is the presence of either a main group or transition metal interstitial atom. In these clusters the valence orbitals of the central atom interact strongly with the radial band of molecular orbitals of the cluster (S_s^σ and P_s^σ/P_p^π in particular) and consequently all the valence electrons of the interstitial atom are considered in the calculation of the polyhedral electron count.³¹

The donation of electron pairs by the ligands into the bonding components of the L_p^π and \bar{L}_p^π bands can be achieved by more than one ligand polyhedron. For example, both $\text{Rh}_4(\text{CO})_{12}$ (3) and $\text{Ir}_4(\text{CO})_{12}$ (4) have tetrahedral metal geometries, but quite different distributions of bridging and terminal carbonyl ligands.³² The compatibility of several co-ordination polyhedra with a given metal geometry is a common feature of metal carbonyl cluster chemistry and is responsible for the stereochemical non-rigidity of the majority of cluster compounds of this type. Since only small energy differences separate alternative structures with differing numbers of terminal and bridging carbonyl ligands, it has not proved possible to provide a general theoretical interpretation of the observed ground state carbonyl configurations in such clusters. Some of the important theoretical and steric factors have been highlighted by Benfield and Johnson,³³ Evans,³⁴ and Minot.³⁵

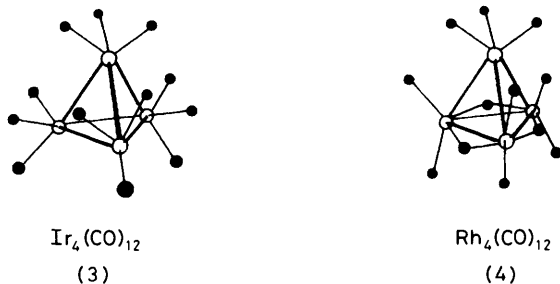
³¹ S. D. Wijesekera and R. Hoffmann, *Organometallics*, 1984, 3, 962.

³² C. H. Wei, *Inorg. Chem.*, 1968, 8, 2384; M. R. Churchill and J. P. Hutchinson, *Inorg. Chem.*, 1978, 17, 3528.

³³ R. E. Benfield and B. F. G. Johnson, *Top. Stereochem.*, 1981, 12, 253.

³⁴ D. G. Evans, *J. Chem. Soc., Chem. Commun.*, 1983, 675.

³⁵ C. Minot and M. Criado-Sancho, *Nouv. J. Chim.*, 1984, 8, 537.



Examples of transition metal carbonyl clusters with *nido*- and *arachno*-geometries have also been isolated and some examples are illustrated in Figure 12. Interestingly, the square anti-prism shown in this Figure can be viewed either as a four-connected polyhedron ($7m + 1$ valence orbitals) or as an *arachno*-bicapped square-antiprism ($7m + 3$ valence orbitals), which has lost two axial capping atoms. $[\text{Ni}_8\text{C}(\text{CO})_{16}]^{2-}$ and $[\text{Co}_8\text{C}(\text{CO})_{18}]^{2-}$ provide specific examples of these alternative situations.³⁶ Similarly, a square-planar cluster can be viewed either as an *arachno*-octahedron (31 valence orbitals) or a saturated ring compound (32 valence orbitals). The two clusters shown in (5) and (6) illustrate these alternative possibilities.³⁷

Clusters where the L_p^π Band is Only Partially Utilized. In the clusters described above there are a sufficient number of bridging and terminal ligands for the bonding components of the $\overline{L_p^\pi}$ and L_p^π bands to be utilized. For clusters where there is either a deficiency of ligands or the metal $d-p$ promotion energies are large then some of the bonding components of the L_p^π band remain empty and the electron count falls below that given in Table 3. The cluster compounds of platinum provide the most extensive series of compounds of this type because the metal $d-p$ promotion energy is particularly large. In mononuclear compounds this large promotion energy is responsible for the formation of a wide range of square-planar 16 electron complexes in preference to trigonal-bipyramidal and square-pyramidal 18 electron complexes. Table 4 summarizes some examples of spherical platinum clusters where the electron count is between four and six electrons fewer than that noted for clusters with identical polyhedral geometries discussed in the previous section.^{38,39} For nickel, where the promotion energies are smaller, there are fewer examples where the electron count diverges significantly from that predicted in the

³⁶ A. Ceriotti, G. Longoni, M. Manasserro, M. Perego, and M. Sansoni, *Inorg. Chem.*, 1985, **24**, 117; V. G. Albano, P. Chini, S. Martinengo, and M. Sansoni, *J. Chem. Soc., Dalton Trans.*, 1978, 463.

³⁷ J. S. Field, R. J. Haines, and D. N. Smit, *J. Organomet. Chem.*, 1982, **224**, C49; H. Vahrenkamp and D. Walter, *Organometallics*, 1982, **1**, 874; J.-F. Halet, R. Hoffmann, and J.-Y. Saillard, *Inorg. Chem.*, 1985, **24**, 1695.

³⁸ D. G. Evans and D. M. P. Mingos, *J. Organomet. Chem.*, 1982, **240**, 321; D. G. Evans and D. M. P. Mingos, *J. Organomet. Chem.*, 1983, **251**, C13.

³⁹ D. Gregson, J. A. K. Howard, M. Murray, and J. L. Spencer, *J. Chem. Soc., Chem. Commun.*, 1981, 716; P. W. Frost, J. A. K. Howard, J. L. Spencer, and D. G. Turner, *J. Chem. Soc., Chem. Commun.*, 1981, 1104.

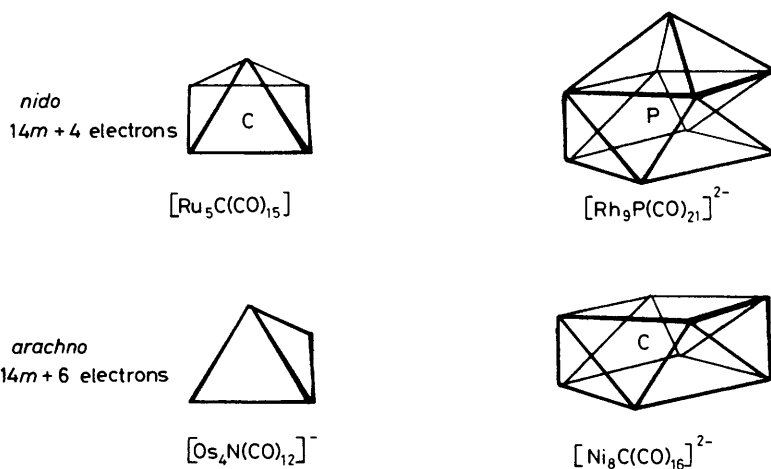


Figure 12 nido- and arachno-Metal carbonyl clusters

Table 4 Examples of platinum cluster compounds where the bonding components of the $L_p^{\sigma}/\bar{L}_p^{\sigma}$ band are only partially filled

Skeletal Geometry	Example	Observed Electron Count	Number of Components of $L_p^{\sigma}/\bar{L}_p^{\sigma}$ Band Not Used
Triangle	$\text{Pt}_3(\text{CO})_3(\text{PR}_3)_3$	42	3
	$\text{Pt}_3(\text{CO})_3(\text{PR}_3)_4$	44	2
Tetrahedron	$\text{Pt}_4\text{H}_8(\text{PR}_3)_4$	56	2
Butterfly	$\text{Pt}_4(\text{CO})_5(\text{PR}_3)_4$	58	2
Trigonal Bipyramid	$\text{Pt}_5\text{H}_8(\text{PR}_3)_5$	68	2
Trigonal Prism	$\text{Pt}_6(\text{CO})_{12}^{2-}$	86	2

previous section. For example, $[\text{Ni}_4(\text{CO})_6(\text{PR}_3)_4]$ has the 60 valence electrons anticipated for the observed tetrahedral geometry, and $[\text{Ni}_6(\text{CO})_{12}]^{2-}$, which has 86 valence electrons, has trigonal antiprismatic geometry that resembles the octahedral geometry found for the isoelectronic $[\text{Co}_6(\text{CO})_{14}]^{4-}$ cluster.⁴⁰ The corresponding $[\text{Pt}_6(\text{CO})_{12}]^{2-}$ cluster has a structure more closely related to a trigonal prism and is based on two nearly eclipsed $\text{Pt}_3(\text{CO})_6$ triangles.⁴¹ The structure of this platinum cluster and the others listed in Table 4 are illustrated in Figure 13. A detailed analysis of the bonding in these platinum clusters has been published elsewhere.³⁸

⁴⁰ J. C. Calabrese, L. F. Dahl, A. Cavalieri, P. Chini, G. Longoni, and S. Martinengo, *J. Am. Chem. Soc.*, 1974, **96**, 2616.

⁴¹ G. Longoni and P. Chini, *J. Am. Chem. Soc.*, 1976, **98**, 7225.

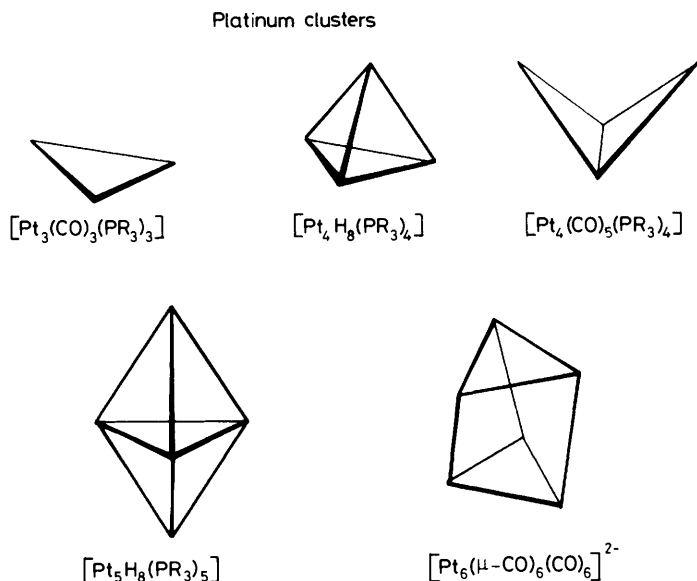
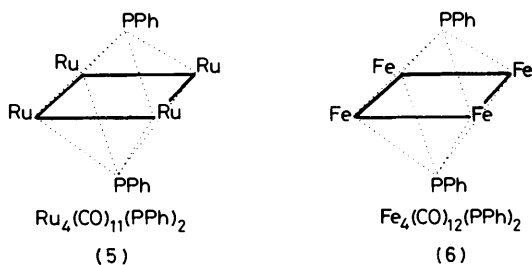


Figure 13 Some examples of platinum clusters



Clusters where the L_p^ Band is Empty.* For the coinage metals, Cu, Ag, and Au, the d band does not make a large contribution to bonding because it has effectively entered into the core.⁴² Furthermore, the band derived from the $(n + 1)p$ valence orbitals do not make a major contribution to bonding because of the large $d-p$ promotion energies. Consequently the major bonding interactions occur through the $(n + 1)s$ valence orbitals. Gold forms the most extensive series of clusters of this type and they have the general formula $[\text{Au}_m(\text{PR}_3)_m]^{*+}$. The lone pairs of the phosphine ligands effectively donate into the L_p^* band generating a set of m metal–ligand bonding molecular orbitals (see Figure 14). Clusters of this type are

⁴² D. M. P. Mingos, *J. Chem. Soc., Dalton Trans.*, 1976, 1163.

characterized by an electron count of $12m + y$, where y represents the number of electrons occupying S_s^σ and components of P_s^σ in Figure 14.⁴³ The number of components of this band which are utilized depends on the cluster nuclearity and geometry. In $[\text{Au}_6(\text{PPh}_3)_6]^{2+}$ (7), which has a geometry based on two tetrahedra sharing a common edge, the S_s^σ and one component of the $P_s^\sigma(P_x^\sigma)$ shell are occupied leading to a y value of four. Whereas in $[\text{Au}_7(\text{PPh}_3)_7]^+$ (8), which has a pentagonal bipyramidal geometry, occupation of S_s^σ and two components of P_s^σ (P_x^σ and P_y^σ) leads to a y value of six. In these low nuclearity clusters the arrangement of metal atoms deviates substantially from spherical and leads to sufficiently large splittings of the P_s^σ manifold for partial occupation to occur.

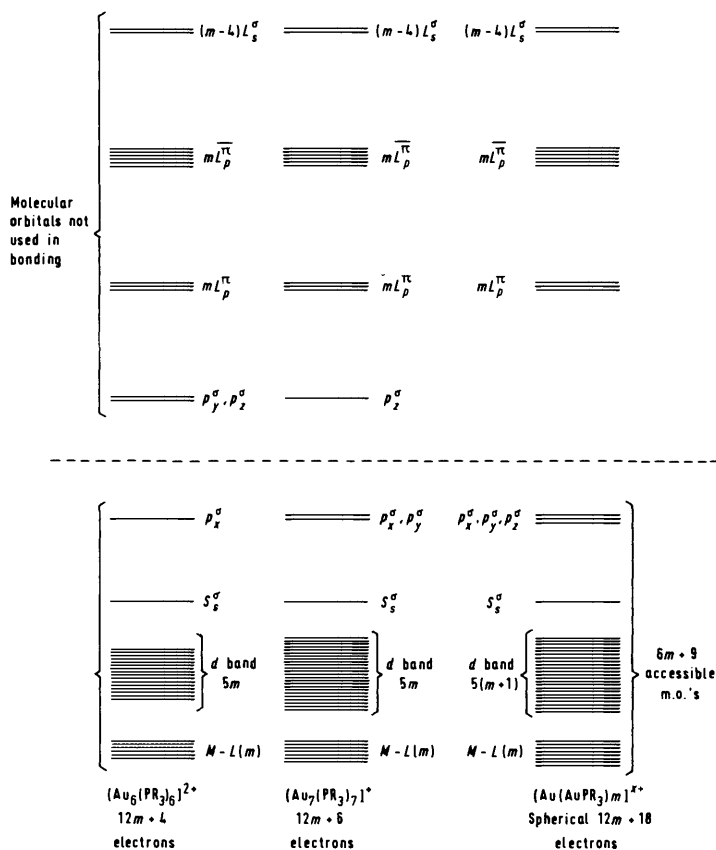
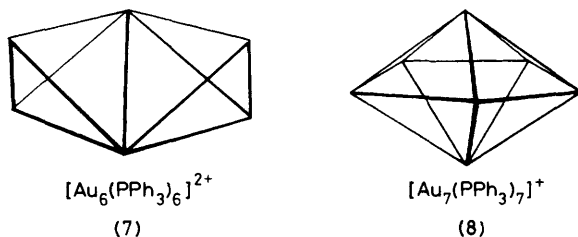


Figure 14 Summary of molecular orbital schemes for gold cluster compounds

⁴³ D. G. Evans and D. M. P. Mingos, *J. Organomet. Chem.*, 1982, **232**, 171.



In the higher nuclearity gold clusters all three components of the P_s^σ manifold are occupied if the metal atoms take up a spherical topology, *i.e.* $x = 8$. In such clusters the radial components of the bonding are enhanced substantially by the presence of an interstitial gold atom. The $6s$ and $6p$ valence orbitals of the central gold atom interact strongly with the S_s^σ and P_s^σ molecular orbitals leading to the set of four very strongly bonding molecular orbitals shown in Figure 14. The interstitial gold atom also has a filled d shell which interacts more weakly with the antibonding D_s^σ components of the L_s^σ band. Occupation of the d band and the four skeletal molecular orbitals S_s^σ and P_s^σ leads to an electron count of $12m + 18$ for the spherical clusters $[\text{Au}(\text{AuPR}_3)_m]^{x+}$. Examples of such cluster compounds are illustrated in Figure 15.

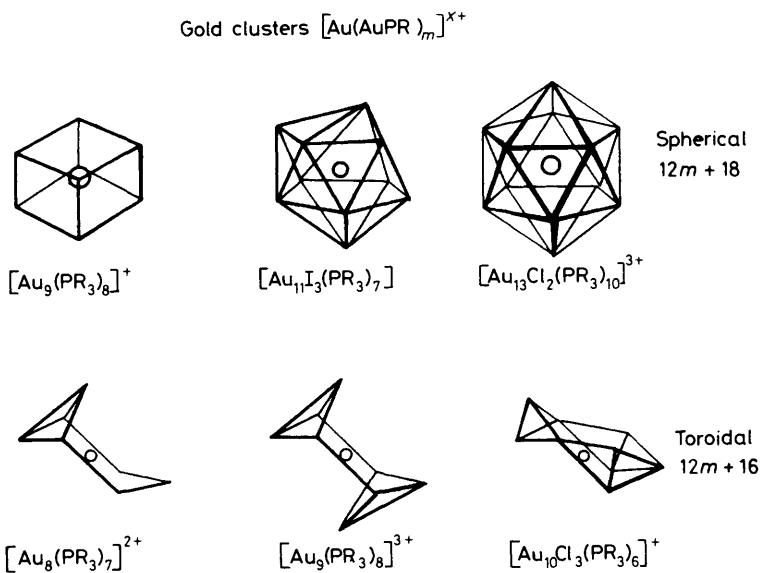


Figure 15 Some examples of spherical and toroidal cluster compounds of gold. All of the clusters have an interstitial gold atom indicated by the central circle

There is a second class of gold cluster compound where only two components of the $P_s\sigma$ band are occupied and therefore they have a total of $12m + 16$ valence electrons. This partial occupation of the $P_s\sigma$ band is made possible by a topological transformation of the cluster geometries. The peripheral metal atoms in such clusters lie on a torus and thereby do not utilize one of the $P_s\sigma$ functions in a bonding fashion. Examples of these toroidal clusters are illustrated in Figure 15.⁴⁴

In these gold clusters the radial bonding effects predominate because the tangential interactions arising from population of the $L_p\pi$ band are not brought into play by bridging ligands. Therefore, the two classes of spherical and toroidal clusters described above bear some resemblance to high co-ordination compounds. This similarity arises not only from the similar electron counting rules, which are summarized below:

Co-ordination Compound ML_m Gold Cluster

Spherical	18 electrons	$12m + 18$ electrons
Square-planar	16 electrons	$12m + 16$ electrons
		toroidal

but also from the observation that the majority of high nuclearity gold cluster compounds are stereochemically non-rigid.

D. Transition Metal Halide and Sulphide Clusters.—For the earlier transition metals the d -band width is greater than 3 eV and therefore the higher lying components of this band are reasonably strongly metal-metal antibonding. In addition, since clusters of these metals are stabilized by halide ligands, there is no opportunity for stabilizing the antibonding components of the d band by back donation effects. Therefore in the clusters $[\text{Mo}_6\text{Cl}_8\text{L}_6]^{4+}$ (9) and $[\text{Ta}_6\text{Cl}_{12}\text{L}_6]^{2+}$ (10)⁴⁵ there are additional inaccessible molecular orbitals derived from the d^8 band. In the face bridged halide cluster $[\text{Mo}_6\text{Cl}_8\text{L}_6]^{4+}$ there is only one inaccessible molecular orbital of a_{2g} symmetry derived from the d^8 band and consequently this cluster has a total of 84 electrons rather than the 86 which is characteristic of metal carbonyl octahedral clusters. In the edge bridged $[\text{Ta}_6\text{Cl}_{12}\text{L}_6]^{2+}$ cluster there are five inaccessible orbitals of t_{2g} and e_u symmetry derived from the d^6 band and consequently this cluster has a total of 76 valence electrons.^{22,46}

When these octahedral clusters are linked into infinite arrays then the partial filling of the d band leads to interesting electrical properties. A more detailed account of the electronic band structures in these infinite solids is beyond the scope of this review.⁴⁷⁻⁴⁹

⁴⁴ K. P. Hall, D. I. Gilmour, and D. M. P. Mingos, *J. Organomet. Chem.*, 1984, **268**, 275.

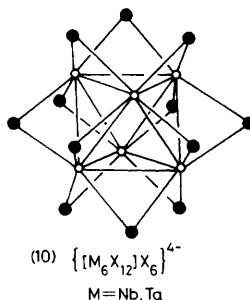
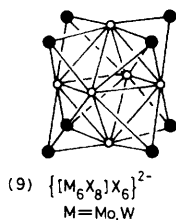
⁴⁵ H. Schäfer and H. G. Schnering, *Angew. Chem., Int. Ed. Engl.*, 1964, **76**, 833; A. Simon, H. G. Schnering, and H. G. Schäfer, *Z. Anorg. Allg. Chem.*, 1965, **339**, 155; 1968, **361**, 235.

⁴⁶ F. A. Cotton and T. E. Haas, *Inorg. Chem.*, 1964, **3**, 10; F. A. Cotton and G. G. Stanley, *Chem. Phys. Lett.*, 1978, **58**, 450.

⁴⁷ T. Hughbanks and R. Hoffmann, *J. Am. Chem. Soc.*, 1983, **105**, 1150.

⁴⁸ J. K. Burdett and J.-H. Lin, *Inorg. Chem.*, 1982, **21**, 5.

⁴⁹ H. Tatawaki, E. Miyoshi, and T. Nakamura, *J. Chem. Phys.*, 1982, **76**, 5073.



E. Summary.—This bonding analysis has emphasized some important similarities in the band structures of main group and transition metal clusters and the following generalizations can be made:

1. Main group and transition metal carbonyl clusters share in common a set of inaccessible molecular orbitals with a high proportion of *p* orbital character. The number and symmetries of the orbitals are directly related to the polyhedral geometry and lead to the electron counting rules summarized in Table 3.

2. The halide clusters of the earlier transition metals have an additional set of inaccessible orbitals which are derived from the d^6 band. The number of antibonding molecular orbitals of this type depends on the locations of bridging ligands in the cluster.

3. The large promotion energies for platinum and gold lead to incomplete utilization of the cluster acceptor orbitals derived from the *p* band and therefore the observed electron counts in clusters derived from these metals falls below that suggested by Table 3. In the gold clusters radial bonding predominates, and in platinum clusters only partial filling of the tangential acceptor orbitals is observed.

4 High Nuclearity Clusters

As the nuclearity of cluster compounds increases the structures begin to resemble the close packed structures of the parent bulk metals more closely. Extensive condensation of tetrahedral and octahedral cluster fragments leads to geometric arrangements of the metals which resemble fragments of the body centred cubic (b.c.c.), hexagonal (h.c.p.), and cubic (c.c.p.) close packed structures that are characteristic of the bulk metals.¹⁸ In addition, close packed arrangements with fivefold symmetry are possible for molecular cluster species and these are described in the subsequent discussion as icosahedral close packed (i.c.p.).

These high nuclearity clusters are approximately spherical and their electronic characteristics can be described according to whether the L_p^n band is fully, partially, or not utilized at all in much the same way as that described above for simpler cluster molecules.⁵⁰ For example, $[Rh_{15}(CO)_{13}]^{3-}$, which has a total of $14m + 2$ valence electrons (198) can be described either as a deltahedron or as a fragment of body centred cubic. These alternative descriptions are illustrated in

⁵⁰ D. M. P. Mingos, *J. Chem. Soc., Chem. Commun.*, 1985, 1352.

Figure 16.⁵¹ In such a cluster the L_p^* band is effectively being utilized by acting as an acceptor to the filled orbitals of the bridging ligands.

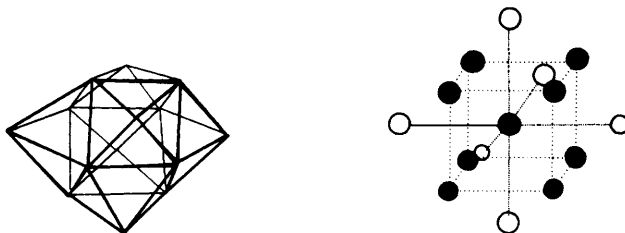


Figure 16 Alternative structural descriptions of $[\text{Rh}_{13}(\text{CO})_{30}]^{3-}$ as a centred deltahedron (left hand side) and as a fragment of a body centred cubic (b.c.c.) metallic lattice (right hand side)

At the other extreme there is an extensive series of cluster compounds where the radial bonding effects predominate and the L_p^* band is effectively empty.⁵² Some examples of these clusters are given in Table 5. It is noteworthy that the majority of examples are based on metals with high $d-p$ promotion energies and the clusters have low ligand:metal ratios. As noted previously in the context of gold cluster compounds (see p. 48), the bonding in such cluster molecules resembles that in high co-ordination compounds. A single interstitial atom filling of the four S_s^{σ} and P_s^{σ} molecular orbitals and the d shell of the interstitial gold atom leads to an electron count of $12n_s + 18$, where n_s is the number of gold atoms which lie approximately on the surface of a sphere. Extension of this model to clusters with several interstitial atoms suggests that the surface atoms act effectively as ligands to the central cluster fragment. It follows that such clusters are characterized by a total of $12n_s + \Delta_i$ electrons, where Δ_i reflects the electronic requirements of the interstitial moiety as defined below.⁵⁰

No. of interstitial atoms	Δ_i	Molecular analogue
1	18	$\text{Mo}(\text{CO})_6$
2	34	$\text{Mn}_2(\text{CO})_{10}$
3	48	$\text{Os}_3(\text{CO})_{12}$
3 (linear)	50	$\text{OsRe}_2(\text{CO})_{14}$
4 (tetrahedral)	60	$\text{Ir}_4(\text{CO})_{12}$
6 (octahedral)	86	$\text{Rh}_6(\text{CO})_{16}$

Examples of clusters which conform to this generalization are summarized in Table 5, and some examples of their structures are illustrated in Figure 17. Given the extreme complexity of the systems the agreement between observed and calculated electron is remarkably good even for the highest nuclearity cluster with 44 metal

⁵¹ J. L. Vidal, L. A. Kapietak, and J. M. Troup, *J. Organomet. Chem.*, 1981, **215**, C11.

⁵² D. M. Washecheck, E. J. Wucherer, L. F. Dahl, A. Ceriotti, G. Longoni, M. Manasserro, M. Sansoni, and P. Chini, *J. Am. Chem. Soc.*, 1979, **101**, 6110; J. L. Vidal, R. C. Schoening, and J. M. Troup, *Inorg. Chem.*, 1981, **20**, 227; B. K. Teo and F. Keating, *J. Am. Chem. Soc.*, 1984, **106**, 2224.

Table 5 Examples of high nuclearity cluster compounds where radial bonding interactions predominate

Compound	Ref.	n_i	n_s	Structure	Electron count		
					observed	calculated	
[Au ₉ (PPh ₃) ₈] ⁺	<i>a</i>	1	8	b.c.c.	114	114	} 12 <i>n_s</i> + 18
[Au ₁₁ I ₃ (PPh ₃) ₇]	<i>b</i>	1	10	b.c.c./i.c.p.	138	138	
[Au ₁₃ Cl ₂ (PMePh ₂) ₁₀] ³⁺	<i>c</i>	1	12	i.c.p.	162	162	
[Pt ₁₉ (CO) ₂₂] ⁴⁻	<i>d</i>	2	17	i.c.p.	238	238	} 12 <i>n_s</i> + 34
[Rh ₂₂ (CO) ₃₅ H _{5-q-m}] ^{q-}	<i>e</i>	2	20	f.c.c./b.c.c.	273 + <i>m</i>	274	
[Au ₁₃ Ag ₁₂ Cl ₆ (PPh ₃) ₁₂] ^{m+}	<i>f</i>	3	22	i.c.p.	317 - <i>m</i>	314	12 <i>n_s</i> + 50 ^{<i>j</i>}
[Pt ₂₆ (CO) ₃₂] ²⁻	<i>g</i>	3	23	h.c.p.	326	324(326)	12 <i>n_s</i> + 48(50) ^{<i>k</i>}
[Ni ₃₈ Pt ₆ (CO) ₄₈ H _{6-m}] ^{m-}	<i>h</i>	6	38	f.c.c.	542	542	} 12 <i>n_s</i> + 86 ^{<i>l</i>}
[Pt ₃₈ (CO) ₄₄ H _{<i>m</i>}] ²⁻	<i>i</i>	6	32	f.c.c.	470 + <i>m</i>	470	

^a J. G. M. van der Linden, M. L. H. Paulissen, and J. E. J. Schmitz, *J. Am. Chem. Soc.*, 1983, **105**, 1903.
^b J. M. M. Smits, P. T. Burskens, J. W. A. van der Velden, and J. J. Bau, *J. Cryst. Spectrosc. Res.*, 1983, **13**, 373. ^c C. E. Briant, B. R. C. Theobald, J. W. White, L. K. Bell, and D. M. P. Mingos, *J. Chem. Soc., Chem. Commun.*, 1981, 201. ^d D. M. Washecheck, E. J. Wucherer, L. F. Dahl, A. Ceriotti, G. Longoni, M. Manasero, M. Sansoni, and P. Chini, *J. Am. Chem. Soc.*, 1979, **101**, 6110. ^e J. L. Vidal, R. C. Schoening, and J. M. Troup, *Inorg. Chem.*, 1981, **20**, 227. ^f B. K. Teo and K. Keating, *J. Am. Chem. Soc.*, 1984, **106**, 2224. ^g D. M. Washecheck, A. Ceriotti, P. Chini, G. Longoni, and L. F. Dahl, personal communication.
^h A. Ceriotti, F. Demartin, G. Longoni, M. Manasero, M. Marchionna, G. Piva, and M. Sansoni, *Angew. Chem.*, in press. ⁱ D. M. Washecheck, A. Ceriotti, M. A. Murphy, D. A. Nagaki, P. Chini, G. Longoni, and L. F. Dahl, personal communication. ^j Linear M₃ interstitial moiety. ^k Triangular M₃ interstitial moiety. Although isolated M₃ clusters are characterized by 48 valence electrons, the presence of bridging metal atoms can lead to the stabilization of an a₂' m.o. and a valence electron count of 50 (D. G. Evans and D. M. P. Mingos, *Organometallics*, 1983, **2**, 435). ^l Octahedral M₆ moiety

atoms. Some of the compounds given in the Table have been incompletely characterized and the generalization provides a basis for estimating either the charge on the cluster or the number of interstitial hydrogen atoms. Interestingly, the observed structures no longer depend on the electron count and fragments of i.c.p., b.c.c., h.c.p., and f.c.c. have been observed. This is consistent with the soft potential energy surface for skeletal rearrangements noted previously for clusters where radial bonding effects predominate. Furthermore, for the bulk metals it is known that only small energy differences separate the alternative close packed structures.^{53,54}

Table 6 gives examples of high nuclearity clusters where partial filling of the L_p^n band occurs. The majority of the examples are derived from rhodium cluster chemistry and they all have a single interstitial atom. The rhodium cluster compounds all have electron counts of $12n_s + 24$ corresponding to the population of the L_p^n band by six electrons. The structures of some of these clusters are illustrated in Figure 18 and underline the lack of a relationship between electron count and skeletal geometry.⁵⁵ Examples with h.c.p., c.c.p., and f.c.c. packing

⁵³ J. K. Burdett, *Prog. Solid State Chem.*, 1985, **15**, 173.

⁵⁴ D. G. Pettifor, *Calphad*, 1977, **1**, 305.

⁵⁵ G. Ciani, A. Sironi, and S. Martinengo, *J. Organomet. Chem.*, 1980, **192**, C42; S. Martinengo, G. Ciani, and A. Sironi, *J. Chem. Soc., Chem. Commun.*, 1980, 1140; S. Martinengo, G. Ciani, A. Sironi, and P. Chini, *J. Am. Chem. Soc.*, 1978, **100**, 7096; G. Ciani, A. Magni, A. Sironi, and S. Martinengo, *J. Chem. Soc., Chem. Commun.*, 1981, 1280; S. Martinengo, G. Ciani, and A. Sironi, *J. Am. Chem. Soc.*, 1980, **102**, 7564.

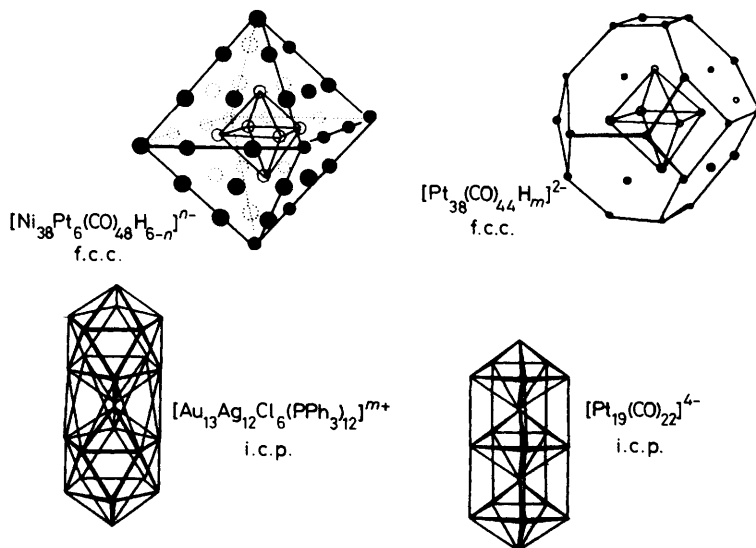


Figure 17 Some examples of high nuclearity clusters where the radial bonding effects predominate

Table 6 Examples of high nuclearity clusters where the tangential bonding interactions make a partial contribution

Compound	Ref.	n_i	n_s	Structure	Electron count	
					observed	calculated
$[\text{Rh}_{14}(\text{CO})_{25}]^{4-}$	<i>a</i>	1	13	b.c.c.	180	180
$[\text{Rh}_{14}(\text{CO})_{26}]^{2-}$	<i>b</i>	1	13	b.c.c.	180	180
$[\text{Rh}_{15}(\text{CO})_{27}]^{3-}$	<i>c</i>	1	14	b.c.c./h.c.p.	192	192
$[\text{Rh}_{17}(\text{CO})_{30}]^{3-}$	<i>d</i>	1	16	h.c.p.	216	216
$[\text{Rh}_{22}(\text{CO})_{37}]^{4-}$	<i>e</i>	1	21	f.c.c./h.c.p.	276	276
$[\text{Pt}_{24}(\text{CO})_{30}]^{2-}$	<i>f</i>	1	23	f.c.c.	302	300

} $12n_s + 24$

^a G. Ciani, A. Sironi, and S. Martinengo, *J. Organomet. Chem.*, 1980, **192**, C42. ^b S. Martinengo, G. Ciani, and A. Sironi, *J. Chem. Soc., Chem. Commun.*, 1980, 1140. ^c S. Martinengo, G. Ciani, A. Sironi, and P. Chini, *J. Am. Chem. Soc.*, 1978, **100**, 7096. ^d G. Ciani, A. Magni, A. Sironi, and S. Martinengo, *J. Chem. Soc., Chem. Commun.*, 1981, 1280. ^e S. Martinengo, G. Ciani, and S. Sironi, *J. Am. Chem. Soc.*, 1980, **102**, 7564. ^f R. A. Montag, A. Ceriotti, and L. F. Dahl, personal communication

arrangements have been observed. The sole example of a platinum cluster in this class has an additional electron pair occupying the $L_p \pi$ band and the reasons for this are not clear at the moment.

From the analysis presented above it is apparent that as the number of interstitial atoms increases the bonding in the cluster becomes increasingly dominated by the radial bonding interactions. This is consistent with the view that for a bare transition metal cluster the tangential molecular orbitals derived from the metal p

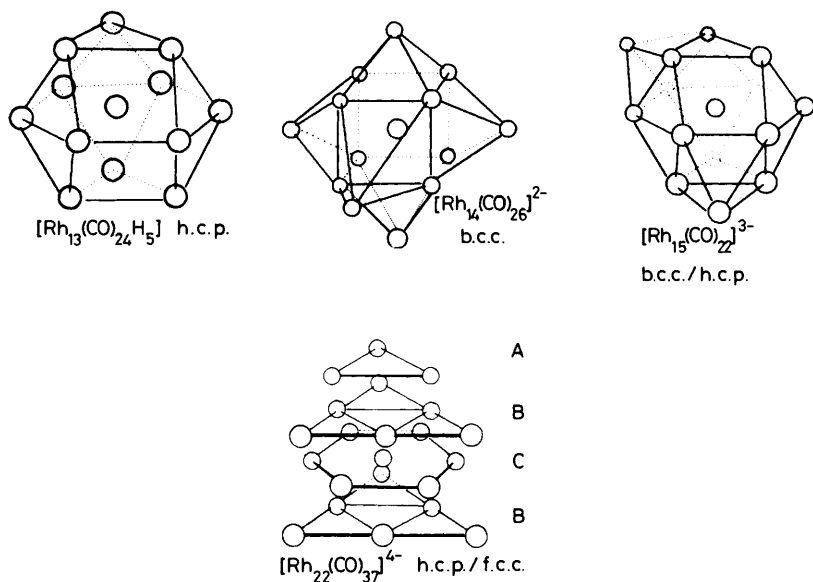


Figure 18 Some high nuclearity rhodium clusters where radial and tangential effects make a contribution to bonding

orbitals cannot enter directly into strong metal–metal bonding but act as acceptors towards ligand orbitals. As the number of interstitial atoms increases the opportunity for such donation effects diminishes and the bonding is dominated increasingly by the d and s orbital interactions. The limiting electron counts in Table 6 correspond to metal–metal bonding occurring primarily through the d and s shells. Formally the clusters have a filled d shell, but it must be emphasized that the bonding in the clusters is of a highly delocalized nature. It involves substantial movements of electron density from the ligands to the cluster and *vice versa*. Therefore it is somewhat problematical to apportion the relative contributions of d , s , and p character in metal–ligand and metal–metal bonds.⁵⁶ The analysis above would suggest that, in general, metal–ligand bonds have a higher proportion of p orbital character and the metal–metal bonds a higher proportion of d orbital character. Furthermore, the fact that the metal–metal bonds have comparable lengths and strengths to those observed for the bulk metal suggests that the final proportions of d , s , and p character associated with the metal atom in a cluster is not too far removed from that in the bulk metal. Definitive experimental evidence supporting this assertion is currently lacking, however.

⁵⁶ R. G. Wooley, *Nouv. J. Chim.*, 1981, **5**, 217; 1981, **5**, 219.

5 Comparison with Band Structure for Bulk Metals

In Figure 19 a schematic illustration of the band structure of a transition metal with a partially filled d shell is shown. The discrete molecular orbitals have been replaced by density of states functions $N(E)$ which represent the number of molecular orbitals with energies in the range E to $E + \delta E$.⁵³ The general features of these bands resemble those discussed above for molecular clusters. The s and p bands which can accommodate a total of eight valence electrons are broad and correspond closely to a free electron description. The d band which can accommodate a total of ten valence electrons is much narrower. Band structure calculations and spectroscopic measurements indicate a substantial degree of overlap between the s and d bands. Therefore maximum metal binding energies are

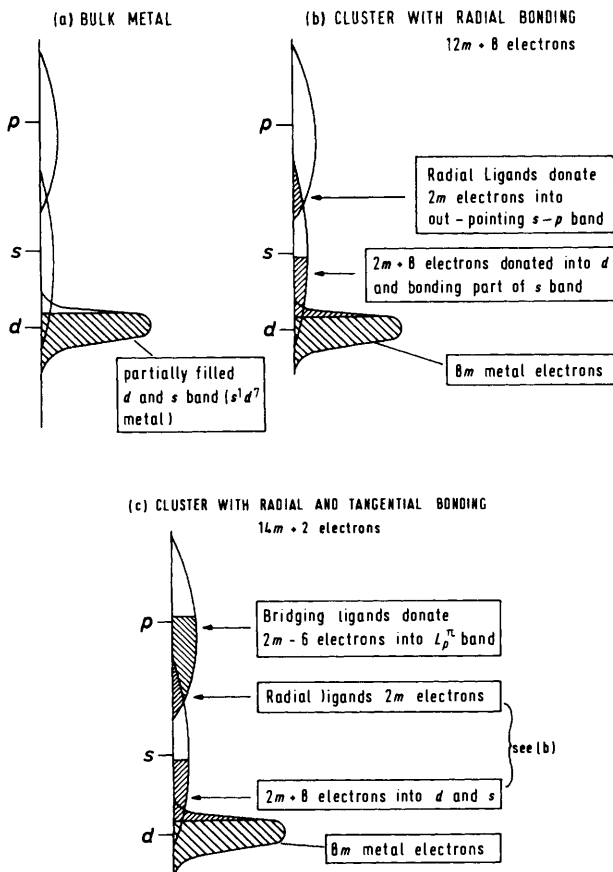


Figure 19 Comparison of band structures for the bulk metal (a), a cluster where only radial bonding effects are important (b), and a cluster where radial and tangential bonding effects contribute (c)

achieved for metals with electronic configurations close to the d^5s^1 half filled situation. The energy differences between alternative close packed structures are not large but a slight preference for b.c.c. is observed for d^4s^1 and d^5s^1 , h.c.p. for d^6s^1 and d^7s^1 , and f.c.c. for d^8s^1 and d^9s^1 , particularly for the second and third row transition metals.^{53,54}

In order to demonstrate the relationship between molecular clusters and the bulk metal, the electronic structure of the former is also represented in a density of states fashion in Figure 19, although they actually have discrete molecular orbitals. In a molecular cluster, electron donation from ligand lone pairs occurs into those components of the d , s , and p bands which are empty and have the suitable nodal characteristics to overlap well with the donor orbitals. For a cluster where radial bonding predominates, e.g. a cluster where the electron count is $12m_s + 18$, the ligands donate $2m$ electrons into outpointing orbitals which occur in the region of overlap between the s and p bands. The cluster bonding occurs primarily through the d shell and the partially filled s shell as shown in Figure 19b. In clusters where radial and tangential bonding effects are important, e.g. in clusters with $14m_s + 2$ valence electrons, then the additional ligands donate into the bonding part of the p band not used in radial bonding (see Figure 19c). Therefore, one can trace in Figures 19c, b, and a the evolution of the electronic structure from molecular cluster into bulk properties and appreciate how the p band is used in a diminishing fashion as the number of ligands is reduced.

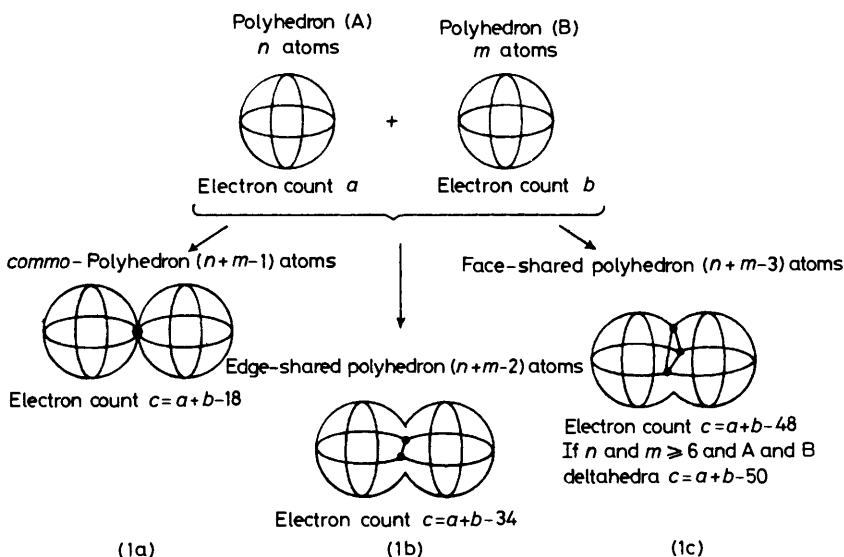


Figure 20 Summary of electron counting rules for condensed polyhedra derived by vertex, edge, and face sharing of simple polyhedral species

6 Intermediate Condensed Clusters

The electronic structures of simple spherical clusters and high nuclearity spherical clusters have been described in the previous sections, but the manner in which cluster growth proceeds has not been described. Since molecular clusters are generally kinetically inert, cluster growth does not proceed in a simple manner whereby successive spherical layers of the cluster are added. It is more probable that the initial stages of growth arise from the loss of either one or two carbonyl ligands and aggregation of the clusters through these centres of co-ordinative unsaturation. This view is supported by the occurrence of numerous cluster compounds whose structures can be described in terms of vertex, edge, and face sharing tetrahedra, octahedra, and trigonal prisms. The electronic structures of these condensed polyhedra can be rationalized in terms of the cluster bonding models developed above^{15,16,57} and their characteristic electron counts are governed by the following simple generalization: *The total electron count in a*

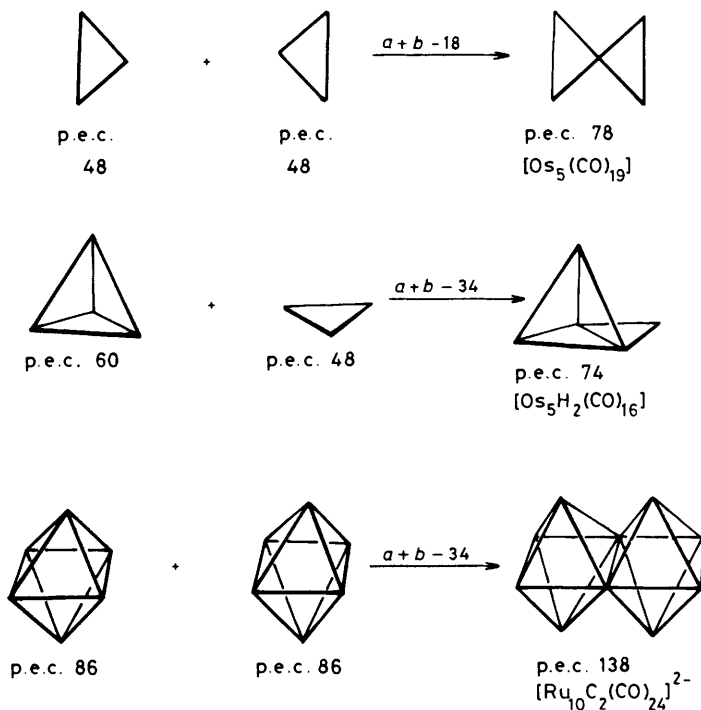


Figure 21 Some simple examples of the application of the condensation rules

⁵⁷ A. J. Stone, *Polyhedron*, 1984, 3, 1298.

condensed cluster is equal to the sum of the electron counts for the parent polyhedra (A) and (B) minus the electron count characteristic of the atom, pair of atoms, or face of atoms common to both polyhedra. This generalization is represented in a pictorial fashion in Figure 20 and some examples of its application are illustrated in Figure 21. A more detailed account of this condensation principle is given in references 15, 16, and 58.

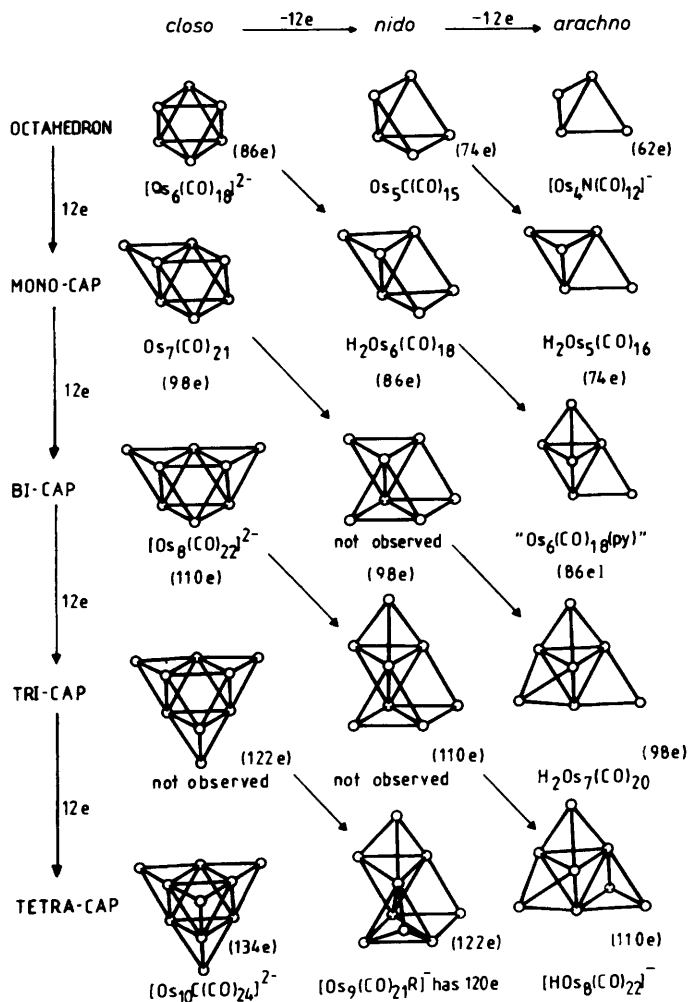


Figure 22 Examples of the growth patterns for osmium cluster compounds based on the capping of the octahedron and its nido- and arachno-derivatives (Adapted from M. McPartlin, *Polyhedron*, 1984, 3, 1279)

⁵⁸ D. M. P. Mingos, *Polyhedron*, 1984, 3, 1289.

The usefulness of this generalization for understanding the growth patterns in cluster chemistry is emphasized by Figure 22 which illustrates the effect of successive capping of simple *closo*-, *nido*-, and *arachno*-clusters derived from the octahedron. Particularly noteworthy is the fact that the resulting tetra-capped octahedron is a fragment of a face centred cubic lattice.^{58,59} It is also significant that capping of the parent polyhedra results in an increment in the electron count of 12. Therefore a polyhedron with n capping atoms has an electron count of $12n$ plus that which is characteristic of the parent polyhedron. In the limit this corresponds to the formula developed in Section 4 for high nuclearity spherical clusters where radial bonding effects predominates, *i.e.* $12n_s + \Delta_i$.

Hence, in this review a consistent bonding model has been developed for clusters that is applicable not only to elements from different parts of the Periodic Table, but also to clusters with 3 to 44 metal atoms. For the lower nuclearity clusters the geometries depend critically on the number of valence electrons, but as the nuclearity increases the condensation generalization permits many alternative structures for a given electron count. Therefore, the potential energy surface connecting the alternative structures becomes progressively soft. For clusters with more than 13 metal atoms the observed structures no longer depend critically on the total numbers of valence electrons, and fragments of b.c.c., f.c.c., h.c.p., and i.c.p. are observed.

Acknowledgement. The S.E.R.C. is thanked for financial support and Mr. Roy Johnston for many helpful discussions.

⁵⁹ M. McPartlin and D. M. P. Mingos, *Polyhedron*, 1984, 3, 1321.